An Analytical Theory of Tropical Cyclone Motion Using a Barotropic Model

ROGER K. SMITH AND WOLFGANG ULRICH

Meteorologisches Institut, Universität München, München, Federal Republic of Germany

(Manuscript received 17 October 1989, in final form 28 February 1990)

ABSTRACT

An analytical theory is presented for the motion of an initially symmetric barotropic vortex on a beta-plane at rest, the prototype problem in the theory of tropical cyclone motion. In the case of vortices with parameter values appropriate to tropical cyclones, the theory shows excellent agreement with equivalent numerical model calculations for a period of between one and two days. In particular, the vortex track and the evolution of vortex asymmetries, the so-called beta gyres, are accurately predicted. The calculations provide further insight into dynamics of tropical cyclone motion in general and provide a firmer basis for interpreting the numerical solutions in particular. They are relevant also to the important problem of designing more appropriate "bogus" vortices for the initialization of dynamically based tropical cyclone forecast models.

1. Introduction

In some of the early theories of tropical cyclone motion, analytical expressions were derived for the initial velocity of the cyclone center, assuming the cyclone to be an initially symmetric vortex in some environmental flow on a beta plane (Sasaki and Miyakoda 1954; Sasaki 1955; Kasahara 1957). The motion was assumed to be governed by the barotropic vorticity equation at some hypothesized "steering level." It was shown that the vortex center moves with a speed close to that of the environmental flow at its center, but with a drift at right angles to and, in the Northern Hemisphere, to the left of the direction of the absolute vorticity gradient of the environmental current. The drift speed is proportional to this gradient and typically only a few kilometers per day.

A more complete and largely analytical theory for motion that took into account the interaction between the vortex and the environmental flow was worked out by Kasahara and Platzman (1963, henceforth referred to as KP). They showed that in addition to the motion characteristics noted above, the vortex is subject also to an initial acceleration in the direction of the absolute vorticity gradient. More recent numerical calculations have shown that this acceleration subsequently overshadows the small predicted drift at right angles to it, leading to a displacement on the order of 100 km in the first 24 hours. However, the direction rapidly deviates from the initial direction predicted by KP's theory. For example, in the absence of an environmental current, a symmetric vortex on a beta plane accelerates northwestwards (southwestwards) rather than polewards in the Northern (Southern) Hemisphere.

The foregoing problem, concerning the motion of an initially symmetric, nondivergent, barotropic vortex on a beta plane with no environmental flow might be viewed as the prototype problem in the theory of tropical cyclone motion. Accordingly, it has been the subject of much recent study, mainly based on numerical model simulations (Chan and Williams 1987; Fiorino and Elsberry 1989; Smith et al. 1990, henceforth referred to as SUD; Shapiro and Ooyama 1990). In the present paper we present a simplified analytical theory for this problem which, hitherto, because of its intrinsically asymmetric nature has been considered intractible.

2. Basic theory

We consider nondivergent barotropic flow on a (nonequatorial) beta plane governed by the vorticity equation

$$\frac{\partial \zeta_*}{\partial t} + u_* \frac{\partial \zeta_*}{\partial x} + v_* \frac{\partial \zeta_*}{\partial y} + \beta v_* = 0, \qquad (2.1)$$

where $\mathbf{u}_* = (u_*, v_*)$ is the velocity vector in a rectangular coordinate system (x, y) which has x pointing eastwards and y pointing northwards; ζ_* is the vertical component of relative vorticity, $\partial v_*/\partial x - \partial u_*/\partial y$; β is the northward derivative of the Coriolis parameter f, and t is the time.

The prototype problem to be studied concerns the motion of an initially symmetric vortex with a prescribed tangential velocity distribution $V(r)$ and corresponding vorticity profile $\zeta(r) = r^{-1} d(rV)/dr$, cen-

Corresponding author address: Prof. Roger K. Smith, Meteorological Institute, University of Munich, Theresienstr. 37 8000 Munich 2, Federal Republic of Germany.

tered at the origin at time $t = 0$, r being the radial distance from the vortex center. It is assumed that there is no environmental flow.

As a preliminary we consider the more general problem when there is an ambient flow $\mathbf{U}(x, y, t)$. Even if this is not present, the vorticity distribution develops asymmetries because of the advection of planetary vorticity by the vortex circulation (e.g., see Kasahara 1957) and one needs to decide whether to regard these asymmetries as part of the distorting vortex, or as part of the environment, in which case the vortex remains symmetric. This so-called partitioning problem was addressed at length by KP who suggested various methods, highlighting the fact that there is no unique solution to the problem. For the present analysis there are advantages to adopting KP's method III in which, by definition, the initial vortex translates unchanged with some velocity $\mathbf{c}(t)$ while all the asymmetries that develop as a result of its interaction with the ambient flow, or with the planetary vorticity field, are considered as part of the ambient flow. One advantage is that all departures from the initial vortex are contained in a single component of the partition, i.e., the ambient flow $\mathbf{U}(x, y, t)$. This partitioning method was used also by SUD. If we let $\mathbf{u}_* = \mathbf{U} + \mathbf{u}$, where $\mathbf{u}$ denotes the symmetric vortex velocity about its center and define $\zeta = \mathbf{k}\cdot\nabla\times\mathbf{u}$, $\Gamma = \mathbf{k}\cdot\nabla\times\mathbf{U}$, where $\mathbf{k}$ is the unit vector in the vertical, then Eq. (2.1) can be partitioned into the two equations

$$\frac{\partial\zeta}{\partial t} + \mathbf{c}(t)\cdot\nabla\zeta = 0, \tag{2.2}$$

and

$$\frac{\partial\Gamma}{\partial t} = -\mathbf{u}\cdot\nabla(\Gamma + f) - (\mathbf{U} - \mathbf{c})\cdot\nabla\zeta - \mathbf{U}\cdot\nabla(\Gamma + f); \tag{2.3}$$

KP devised a variational method to determine $\mathbf{c}(t)$, while SUD took this to be the rate of displacement of the position of maximum relative vorticity in the flow.

The simplification of (2.3) leading to a tractable analytical problem for the vortex motion was guided strongly by the numerical calculations of SUD. These authors showed that, in the absence of a basic flow, the vorticity changes are dominated by the terms in Eq. (2.2); i.e. to a first approximation the local vorticity change is essentially determined by the advection of the vortex vorticity with velocity $\mathbf{c}$ (SUD, Fig. 6). Furthermore, $\mathbf{c}$ is to a close approximation equal to the environmental flow velocity at the vortex center and $|\mathbf{U} - \mathbf{c}|$ is relatively small ($<\frac{1}{4}|\mathbf{c}|$) over much of the vortex (SUD, Fig. 8). But $\mathbf{U}$ is related to the environmental vorticity, the time evolution of which is determined by Eq. (2.3). SUD found also that to a surprisingly good first approximation, the vortex asymmetries governed by this equation can be determined by neglecting the motion of the vortex and calculating Γ on the assumption that its rate of change is associated with the advection of absolute environmental vorticity ($\Gamma + f$) by the vortex circulation; i.e.

$$\frac{\partial\Gamma}{\partial t} = -\mathbf{u}\cdot\nabla(\Gamma + f). \tag{2.4}$$

This result is contrary to what one would deduce from a scale analysis of Eq. (2.3), which would suggest that the term $-(\mathbf{U} - \mathbf{c})\cdot\nabla\zeta$ is the dominant term contributing to $\partial\Gamma/\partial t$. The scale analysis is nevertheless worth considering.

Following KP we take length and velocity scales L_E, U_E and L_V, U_V for the environment and the vortex, respectively, and obtain the following relative sizes of terms on the right hand side of (2.3):

$$\frac{U_V}{U_E} \quad \frac{U_V}{\beta L_V^2} \quad 1,$$

where we have assumed that $|\nabla\Gamma| \leqslant \beta$, implying that $L_E \geqslant (U_E/\beta)^{1/2}$. Taking typical values $U_E = 2$ m s^{-1}, $L_V = 50$ km, $U_V = 50$ m s^{-1} and $\beta = 2\times10^{-11}$ m^{-1} s^{-1} (a tropical value), then $L_E \geqslant 300$ km and estimates for these ratios are:

$$25 \quad 1000 \quad 1,$$

suggesting that the second term is of over-riding importance. These estimates are naive for two reasons. First, as noted above, $|\mathbf{U} - \mathbf{c}| \ll \max[|\mathbf{U}|, |\mathbf{c}|]$ across the vortex core so that estimate of 1000 is likely to be a gross overestimate for the second term (note that $|\nabla\zeta|$ is relatively large in the vortex core while $|\mathbf{U} - \mathbf{c}|$ is relatively small so that the actual magnitude of this term is difficult to precisely diagnose in numerical calculations because of inaccuracies in determining $\mathbf{c}$). Second, in the present method of partitioning, the environmental vorticity field includes the vortex scale asymmetries and, as shown by SUD, the shearing effect of the strong angular shear leads to progressively fine scale structure in this field (e.g., see SUD, Fig. 9). These two factors are obstacles to a meaningful scale analysis and in the theory to be presented we have been guided by insights derived from the numerical calculations.

For the reasons given above, the diagnostic of the second term on the right of (2.3) from the numerical model is unreliable, but the calculations in general point to the dominance of the first term in determining the vortex asymmetries. Consistent with the scale analysis, the third term is not appreciable. Indeed, if the terms in (2.3) are interpreted so that $\partial/\partial t$ is measured relative to the moving vortex, then $\mathbf{U}$ must be replaced by $\mathbf{U} - \mathbf{c}$ in the last term on the right hand side. This reduces the magnitude of this term in the region of the vortex where $\mathbf{U} \approx \mathbf{c}$, but may increase its size at large radii if, for example $|\mathbf{U}| \to \mathbf{0}$ there, as in the prototype problem.

Guided by the results of SUD, we assume that, in the prototype problem (where $\mathbf{U}(x, y, 0) = \mathbf{0}$), Eq.

(2.3) can be approximated by (2.4), implying that local relative vorticity changes are due to advection of absolute vorticity by the vortex. In cylindrical coordinates (r, θ) centered on the vortex center, Eq. (2.4) may be written as

$$\left[\frac{\partial}{\partial t} + \Omega(r)\frac{\partial}{\partial \theta}\right](\Gamma + f) = 0, \tag{2.5}$$

where $\Omega(r) = V(r)/r$ is the angular rotation rate of the tangential motion. Assuming that $\Gamma \equiv 0$ at $t = 0$, this equation is easily integrated[1] to give the environmental vorticity at time t,

$$\Gamma_a(r, \theta, t) = \zeta_1(r, t)\cos\theta + \zeta_2(r, t)\sin\theta, \tag{2.6}$$

where

$$\zeta_1 = -\beta r \sin\{\Omega(r)t\}, \tag{2.7a}$$

$$\zeta_2 = -\beta r[1 - \cos\{\Omega(r)t\}]. \tag{2.7b}$$

The streamfunction corresponding to this asymmetry satisfies the Poisson equation $\nabla^2\Psi_a = \Gamma_a$, with Dirichlet boundary condition $\Psi_a \to 0$ as $r \to \infty$ and it readily follows that

$$\Psi_a(r, \theta, t) = \Psi_1(r, t)\cos\theta + \Psi_2(r, t)\sin\theta, \tag{2.8}$$

where for $n = 1, 2$,

$$\Psi_n(r, t) = -\frac{r}{2}\int_r^\infty \zeta_n(p, t)dp - \frac{1}{2r}\int_0^r p^2\zeta_n(p, t)dp. \tag{2.9}$$

The Cartesian velocity components U_a, V_a $(= -\partial\Psi_a/\partial y, \partial\Psi_a/\partial x)$ are given by

$$U_a = \cos\theta\sin\theta\left[\frac{\Psi_1}{r} - \frac{\partial\Psi_1}{\partial r}\right] - \sin^2\theta\frac{\partial\Psi_2}{\partial r} - \cos^2\theta\frac{\Psi_2}{r}, \tag{2.10a}$$

$$V_a = \cos^2\theta\frac{\partial\Psi_1}{\partial r} + \sin^2\theta\frac{\Psi_1}{r} - \cos\theta\sin\theta\left[\frac{\Psi_2}{r} - \frac{\partial\Psi_2}{\partial r}\right]. \tag{2.10b}$$

In order that these expressions give a unique velocity at the origin, they must be independent of θ as $r \to 0$, in which case

$$\left.\frac{\partial\Psi_n}{\partial r}\right|_{r=0} = \lim_{r\to 0}\frac{\Psi_n}{r}, \quad (n = 1, 2),$$

and using (2.9) it follows that

$$\left.\frac{\partial\Psi_n}{\partial r}\right|_{r=0} = -\frac{1}{2}\int_0^\infty \zeta_n(p, t)dp. \tag{2.11}$$

[1] See also SUD, Eqs. (4.1)–(4.3).

If we make the reasonable assumption that the symmetric vortex moves with the velocity of the asymmetric flow across its center, the vortex speed is simply

$$\mathbf{c}(t) = \left[-\left.\frac{\partial\Psi_2}{\partial r}\right|_{r=0}, \left.\frac{\partial\Psi_1}{\partial r}\right|_{r=0}\right], \tag{2.12}$$

which can be evaluated using (2.11).

The assumption is reasonable because *at the vortex center* $\zeta_* \gg f$ and the governing equation (2.1) expresses the fact that $\zeta_* + f$ is conserved following the motion. Since the symmetric circulation does not contribute to advection across the vortex center, advection must be by the asymmetric component and with the KP method of partitioning, this is simply the environmental flow by definition. The slight error committed in supposing that ζ_* is conserved rather than $\zeta_* + f$ is equivalent to neglecting the propagation of the vortex center as described by the early initial motion theories (Sasaki and Miyakoda 1954; Sasaki 1955; Kasahara 1957). The track error amounts to no more than a few kilometers per day which is negligible compared with actual vortex displacements (e.g., see Fig. 5).

The vortex track $\mathbf{X}(t) = [X(t), Y(t)]$ may be obtained by integrating the equation $d\mathbf{X}/dt = \mathbf{c}(t)$, whereupon, using (2.11) and (2.12),

$$\begin{bmatrix} X(t) \\ Y(t) \end{bmatrix} = \begin{bmatrix} \frac{1}{2}\int_0^\infty \left\{\int_0^t \zeta_2(p, t)dt\right\}dp \\ -\frac{1}{2}\int_0^\infty \left\{\int_0^t \zeta_1(p, t)dt\right\}dp \end{bmatrix}. \tag{2.13}$$

Using (2.7), this expression reduces to

$$\begin{bmatrix} X(t) \\ Y(t) \end{bmatrix} = \begin{bmatrix} -\frac{1}{2}\beta\int_0^\infty r\left[t - \frac{\sin\{\Omega(r)t\}}{\Omega(r)}\right]dr \\ \frac{1}{2}\beta\int_0^\infty r\left[\frac{1 - \cos\{\Omega(r)t\}}{\Omega(r)}\right]dr \end{bmatrix}, \tag{2.14}$$

which determines the vortex track in terms of the initial angular velocity profile of the vortex.

To illustrate the solutions we choose the vortex profile used by SUD so that we can compare the model results with their numerical solutions. The velocity profile $V(r)$ and corresponding angular velocity profile $\Omega(r)$ are shown as solid lines in Fig. 1. The velocity profile is approximately the same as that used by Chan and Williams (1987); the maximum wind speed of 40 m s^{-1} occurs at a radius of 100 km and the region of gale force winds (>15 m s^{-1}) extends to 300 km. The angular velocity has a maximum at the vortex center and decreases monotonically with radius. Figure 2 shows the asymmetric vorticity field calculated from (2.6) and the corresponding streamfunction field from (2.8) at selected times, while Fig. 3 compares the analytical solutions with numerical solutions at 24 hours.

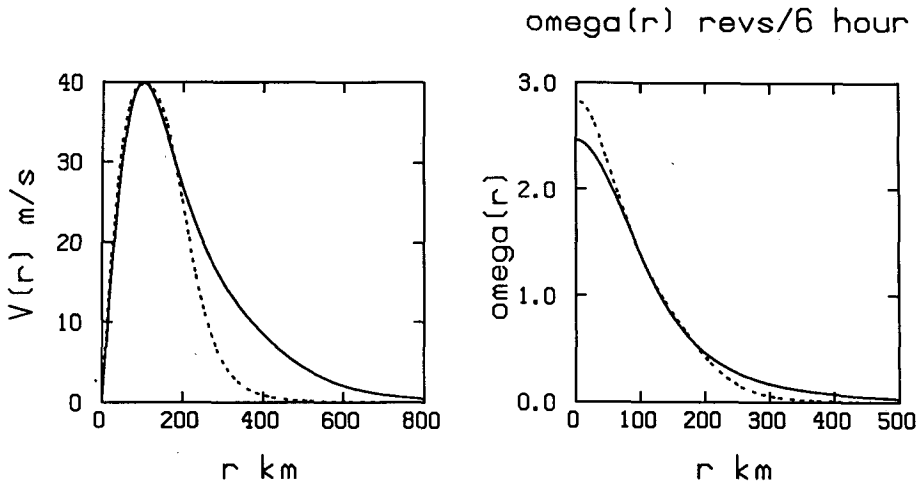

FIG. 1. (a) Tangential velocity profile $V(r)$ and (b) angular velocity profile $\Omega(r)$ for the symmetric vortex. Solid lines are for the standard vortex used by SU. Dashed lines are for a smaller vortex with the same functional form, but for which $V = 5$ m s^{-1} at $r = 300$ km.

The integrals involved are calculated using simple quadrature. After one minute the asymmetric vorticity and streamfunction fields show an east–west oriented dipole pattern as predicted in the early "initial motion" theories (e.g., Adem 1956; Kasahara 1957). The vorticity maxima and minima occur at the radius of maximum tangential wind and there is a southerly component of the asymmetric flow across the vortex center (Fig. 2a). As time proceeds, the vortex asymmetry is rotated by the symmetric vortex circulation and its strength and scale increase for reasons discussed by SUD. In the inner core (typically $r < 200$ km), the asymmetry is rapidly sheared by the relatively large radial gradient of Ω (Fig. 1b). In response to these vorticity changes, the streamfunction dipole strengthens and rotates also, whereupon the asymmetric flow across the vortex center increases in strength and rotates northwestwards. Even at 24 hours, the asymmetric vorticity and streamfunction patterns show remarkable similarity to those diagnosed from the complete numerical solution (Fig. 3). Nevertheless, the small differences in detail between the vorticity patterns are manifest in a more westerly oriented streamflow across the vortex center in the analytical solution and these are reflected in differences in the vortex tracks (see below). It should be noted that the numerical model simulations are for a zonal channel with impervious northern and southern boundaries. However, we have found that the differences in boundary conditions do not account for the differences in the streamfunction patterns shown in Fig. 3 which show only a part of the 2000 km × 2000 km domain used for the numerical calculations. In section 3 we show that the principle differences at this time are due to the neglect of the term $-(\mathbf{U} - \mathbf{c}) \cdot \nabla \zeta$ in calculating the vorticity field in the analytical model.

The evolution of the streamfunction asymmetry in the numerical model was studied by Fiorino and Elsberry (1989) and by SUD. The foregoing analytical solution and comparisons show that the asymmetry is dominated by *a pair of* orthogonal dipoles with different radial profiles and strengths and that these profiles evolve with time. These profiles, characterized by the functions $\Psi_n(r, t)$ in Eq. (2.8), are shown in Fig. 4 at 24 hours.

Figure 5 shows the track of the analytical vortex over a 48 hour period compared with that in the numerical solution, which can be regarded as the control case. The track calculation was performed on a 4000 km × 4000 km domain with a 20 km grid size. It follows that the analytical solution gives a track that is too far westward, but the average speed of motion is comparable with, but a fraction smaller than in the control case for this entire period. However, one must expect the analytical solution to deteriorate after 24 hours (SUD, see especially Fig. 5).

While the overall agreement between the analytical and numerical results is remarkable considering the simplicity of the theory, the discrepancy in the track direction even at early times calls for an explanation. Moreover, comparisons for a smaller scale vortex in which the tangential velocity reduces to only 5 m s^{-1} at 300 km radius (the dashed profile in Fig. 1a) do not compare so favorably. Indeed, there is a significant discrepancy in the evolution of the vortex asymmetry between the analytical and numerical solutions, even after only 3 hours of integration (Fig. 6), and also between the tracks (Fig. 7). For example, according to the discussion in section 4 of SUD, the axis of the asymmetric gyres should rotate cyclonically with time, but examination of the gyre structure in the numerical simulation shows that, after a short period of time, this axis

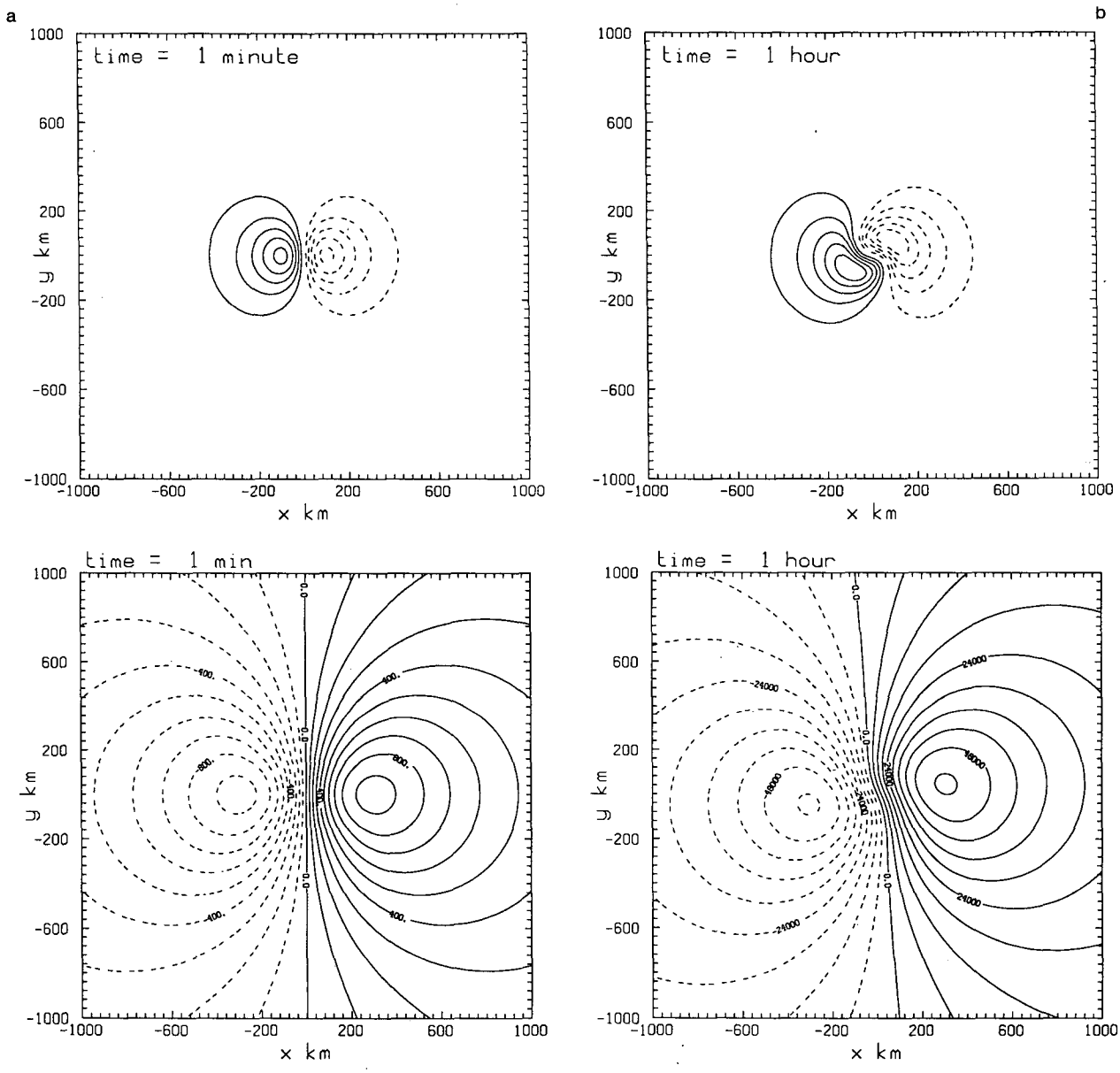

FIG. 2. Asymmetric vorticity (top panels) and streamfunction fields (bottom panels) at selected times: (a) 1 min, (b) 1 hour, (c) 3 hours, (d) 12 hours. Contour intervals for Γ_a are: 1×10^{-8} s^{-1} in (a), 5×10^{-7} s^{-1} in (b), 1×10^{-6} s^{-1} in (c) and 2×10^{-6} s^{-1} in (d). Coutour intervals for Ψ_a are: 100 m^2 s^{-1} in (a), 6×10^3 m^2 s^{-1} in (b), 1×10^4 m^2 s^{-1} in (c) and 5×10^4 m^2 s^{-1} in (d).

retrogresses. At first sight this seems to imply a retrograde propagation of the wavenumber one asymmetry as a type of centrifugal wave on the vortex core. Such an effect would seem likely to be more pronounced for a vortex that decays more rapidly with radius where the radial gradient of relative vorticity is larger. However, a study of wave propagation on a barotropic vortex by Gent and McWilliams (1986) has shown that while a wavenumber one mode is stable, it has zero frequency; i.e., it does not retrogress relative to the vortex. Nevertheless, it is conceivable that such a wave could be forced as a result of vortex motion as suggested by Carr and Williams (1989). We explore this idea in the following section and show how the foregoing discrepancies between the analytical and numerical theories may be resolved.

3. Refinements to the theory

As a preliminary, it is insightful to consider the vorticity equation governing small perturbations to a *stationary* symmetric vortex again with tangential velocity

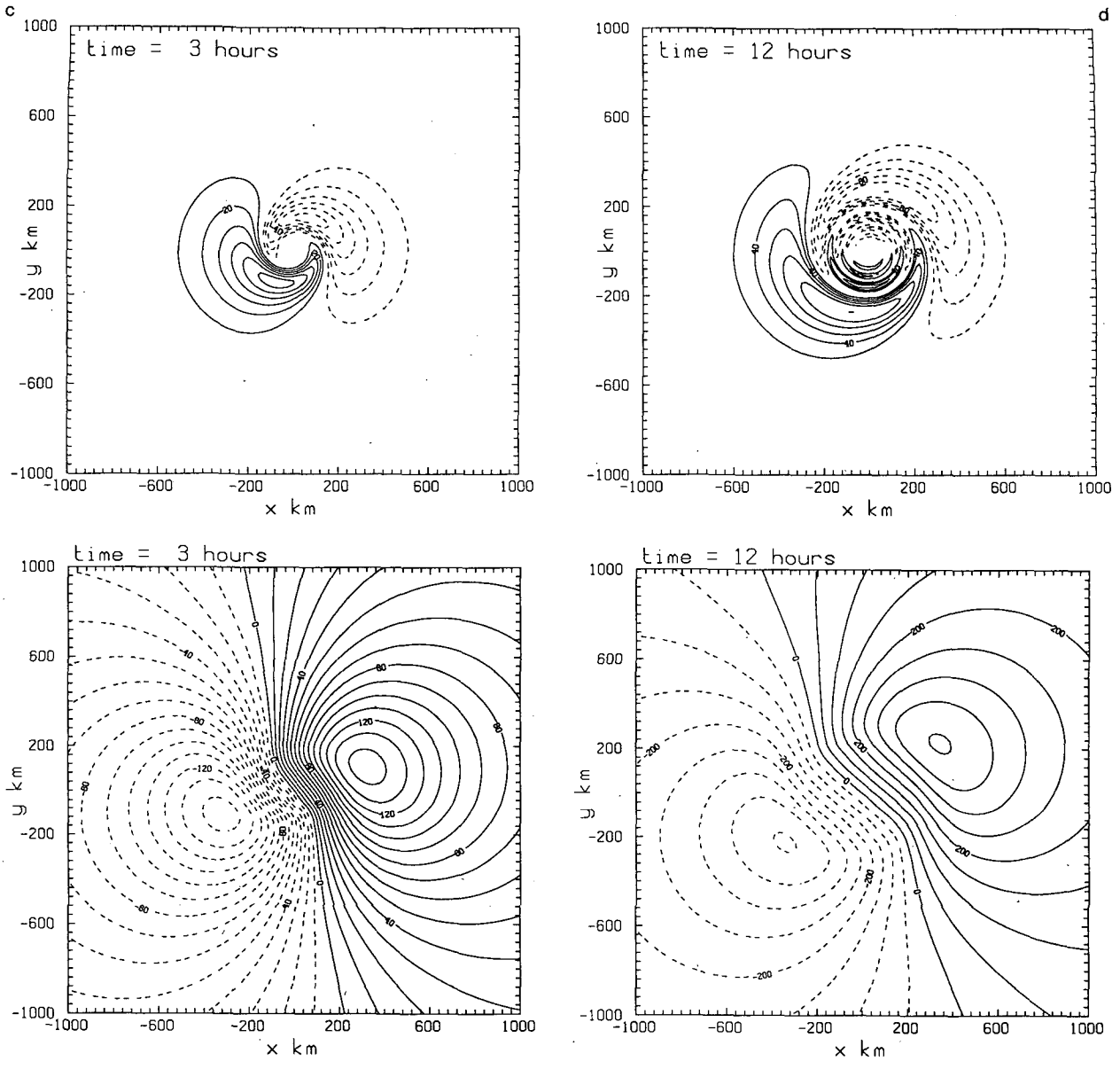

FIG. 2. (*Continued*)

distribution $V(r)$, *on a β-plane.* If the velocity perturbation is $\mathbf{u}' = (u', v')$ in cylindrical coordinates (r, θ), the perturbation vorticity $\zeta' = (1/r)(\partial(rv')/\partial r - \partial u'/\partial\theta)$ satisfies the equation

$$\frac{\partial\zeta'}{\partial t} + \frac{V}{r}\frac{\partial\zeta'}{\partial\theta} + u'\frac{d\bar{\zeta}}{dr} - \beta V\cos\theta + \beta\mathbf{u}'\cdot\mathbf{j} = 0, \quad (3.1)$$

where $\mathbf{j}$ is a unit vector in the northward direction and $\bar{\zeta} = r^{-1}\partial(rV)/\partial r$ is the relative vorticity of the basic vortex. An alternative form of (3.1) is

$$\left(\frac{\partial}{\partial t} + \frac{V}{r}\frac{\partial}{\partial\theta}\right)(\zeta' + f) = -u'\frac{d\bar{\zeta}}{dr} - \beta\mathbf{u}'\cdot\mathbf{j}. \quad (3.2)$$

It is illuminating to compare this with Eq. (2.3) rewritten in the form

$$\left(\frac{\partial}{\partial t} + \mathbf{u}\cdot\nabla\right)(\Gamma + f) = -(\mathbf{U} - \mathbf{c})\cdot\nabla\zeta - (\mathbf{U} - \mathbf{c})\cdot\nabla(\Gamma + f), \quad (3.3)$$

appropriate to a frame of reference moving with the vortex (hence the addition of the term $\mathbf{c}\cdot\nabla(\Gamma + f)$ on the right hand side). Clearly, if (3.2) is considered in the frame reference moving with the vortex, $\Gamma + f$ can be identified in the linear problem with $\zeta' + f$ and $(\mathbf{U} - \mathbf{c})\cdot\nabla$ with $u'd/dr$, etc. [note that $\mathbf{u}$ refers to the

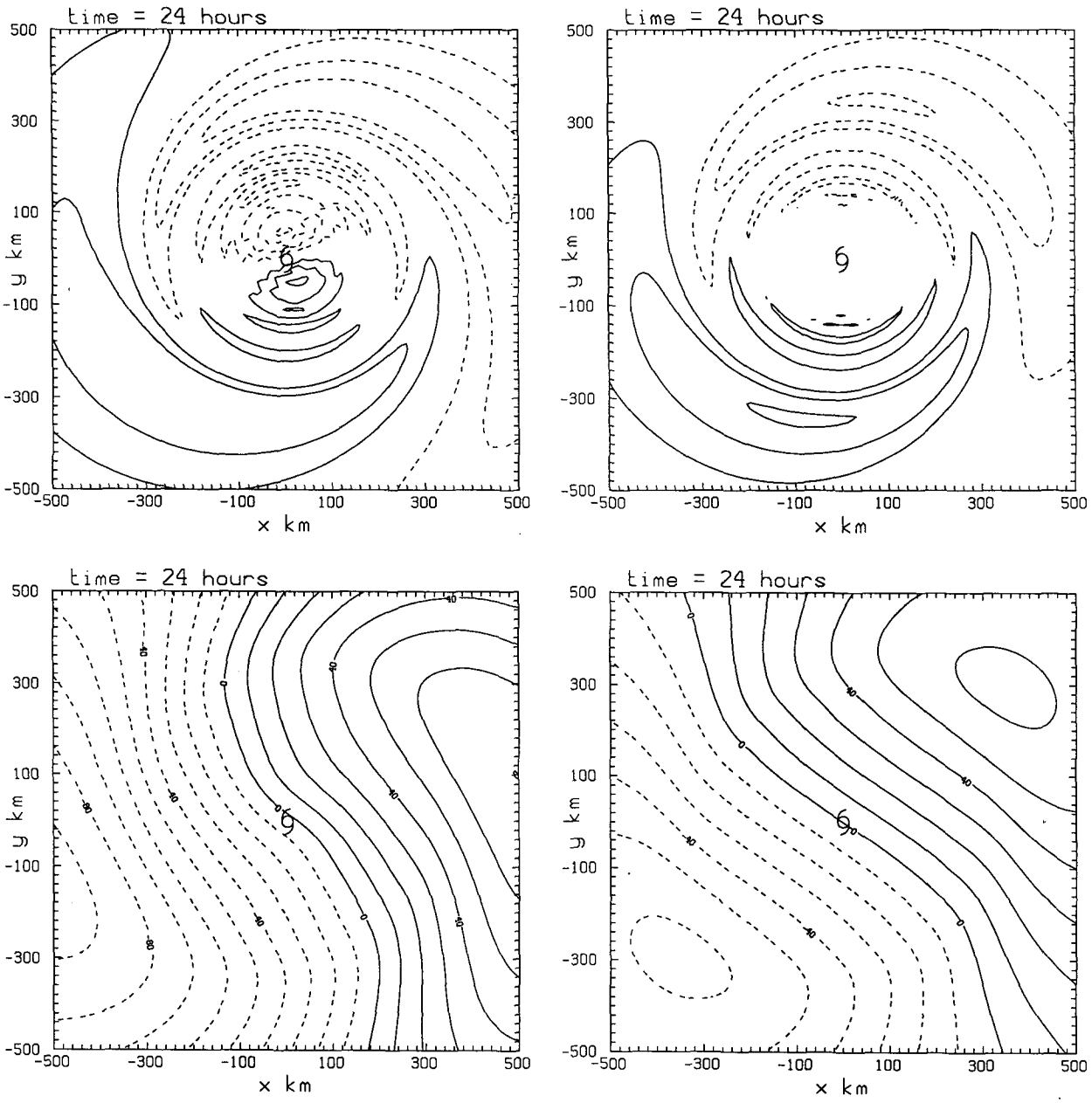

FIG. 3. Comparison of the analytically computed asymmetric vorticity and streamfunction fields (upper right and lower right) with those for the corresponding numerical solutions at 24 hours. Only the inner part of the numerical domain, centered on the vortex center, is shown (the calculations were carried out on a 2000 km × 2000 km domain). Contour intervals are 5×10^{-6} s^{-1} for Γ_a and 10^5 m^2 s^{-1} for Ψ_a. The tropical cyclone symbol represents the vortex center.

symmetric vortex whereupon $\mathbf{u}\cdot\nabla \equiv (V/r)(\partial/\partial\theta)]$. A similar approach is contained in a recent study of vortex motion by Willoughby (1988). Consistent with the naive scale analysis of the preceding section the numerical calculations suggest that the term $-(\mathbf{U}-\mathbf{c})\cdot\nabla\zeta$ is the dominant one on the right-hand side of Eq. (3.3) and its contribution to the asymmetric vorticity distribution Γ_{ac} may be estimated using the zero order solution Γ_a given in that section. The analysis is as follows.

Writing $\Gamma = \Gamma_a + \Gamma_{ac}$ and $\mathbf{U} = \mathbf{U}_a$ in (3.3) and neglecting the last term therein, we obtain using (2.4) an equation to the *asymmetric* vorticity field Γ_{ac}:

$$\frac{\partial \Gamma_{ac}}{\partial t} + \mathbf{u}\cdot\nabla\Gamma_{ac} = -(\mathbf{U}_a - \mathbf{c})\cdot\nabla\zeta. \qquad (3.4)$$

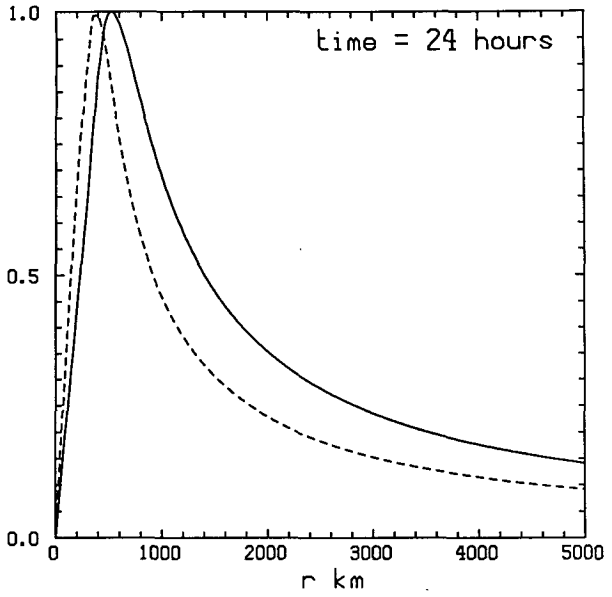

FIG. 4. Radial profiles of $\Psi_n/\Psi_{n\max}$ ($n = 1, 2$) at 24 hours where $\Psi_{n\max}$ is the maximum absolute value of Ψ_n. Solid line is Ψ_1, dashed line is Ψ_2. Here, $\Psi_{1\max} = 4.8 \times 10^5$ m^2 s^{-1}; $\Psi_{2\max} = 4.2 \times 10^5$ m^2 s^{-1}.

The asymmetric flow $\mathbf{U}_a$ is obtained from (2.10) and $\mathbf{c}$ from (2.12) and we can calculate the streamfunction Ψ'_a of the *vortex-relative* flow $\mathbf{U}_a - \mathbf{c}$, from

$$\Psi'_n = \Psi_a - \Psi_c,$$

where

$$\Psi'_c = r(V_a \cos\theta - U_a \sin\theta)$$
$$= r\left[\left.\frac{\partial \Psi_1}{\partial r}\right|_{r=0} \cos\theta + \left.\frac{\partial \Psi_2}{\partial r}\right|_{r=0} \sin\theta\right]. \quad (3.5)$$

Then, using (2.8), (2.9), (2.11) and (3.5) we obtain

$$\Psi'_a = \Psi'_1(r, t) \cos\theta + \Psi'_2(r, t) \sin\theta, \quad (3.6)$$

where

$$\Psi'_n(r, t) = \Psi_n - r\left[\frac{\partial \Psi_n}{\partial r}\right]_{r=0}, \quad (n = 1, 2)$$
$$= \frac{1}{2} r \int_0^r \left(1 - \frac{p^2}{r^2}\right) \zeta_n(p, t) dp. \quad (3.7)$$

After a little algebra it follows using (2.10)–(2.12) and (3.7) that

$$-(\mathbf{U}_a - \mathbf{c}) \cdot \nabla \zeta = \chi_1(r, t) \cos\theta + \chi_2(r, t) \sin\theta, \quad (3.8)$$

where

$$\begin{bmatrix} \chi_1(r, t) \\ \chi_2(r, t) \end{bmatrix} = \frac{1}{r} \frac{d\zeta}{dr} \times \begin{bmatrix} \Psi'_2(r, t) \\ -\Psi'_1(r, t) \end{bmatrix}. \quad (3.9)$$

After a little algebra, outlined in Appendix A, it follows that

$$\Gamma_{ac}(r, \theta, t) = \zeta_{1c}(r, t) \cos\theta + \zeta_{2c}(r, t) \sin\theta, \quad (3.10)$$

where

$$\zeta_{nc}(r, t) = \int_0^t \chi_n(r, t) dt$$
$$= -\frac{1}{2} \beta \frac{d\zeta}{dr} \int_0^r p\left(1 - \frac{p^2}{r^2}\right) \eta_n(r, p, t) dp, \quad (3.11)$$

and

$$\eta_1(r, p, t) = \frac{\sin\{\Omega(r)t\}}{\Omega(r)} - \frac{\sin\{\Omega(r)t\} - \sin\{\Omega(p)t\}}{\Omega(r) - \Omega(p)}, \quad (3.12a)$$

$$\eta_2(r, p, t) = \frac{1 - \cos\{\Omega(r)t\}}{\Omega(r)} + \frac{\cos\{\Omega(r)t\} - \cos\{\Omega(p)t\}}{\Omega(r) - \Omega(p)}. \quad (3.12b)$$

The integrals in (3.11) can be readily evaluated using quadrature.

Figure 8 shows the pattern of relative streamlines at 24 hours for the larger vortex in Fig. 1 and Fig. 9a shows the correction to the asymmetric vorticity field at this time. The relative streamflow across the vortex core is weak as corroborated by the numerical solution

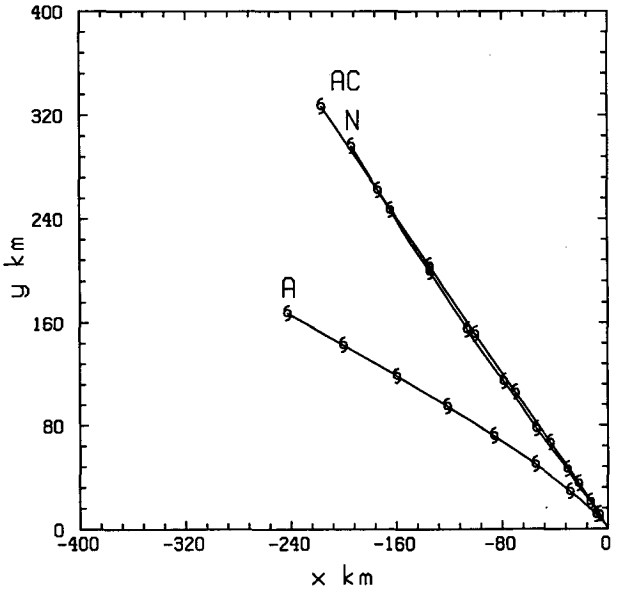

FIG. 5. Comparison of the analytically calculated vortex track (denote by A) compared with that for the corresponding numerical solution (denote by N). The track by AC is the analytically corrected track referred to in §3.

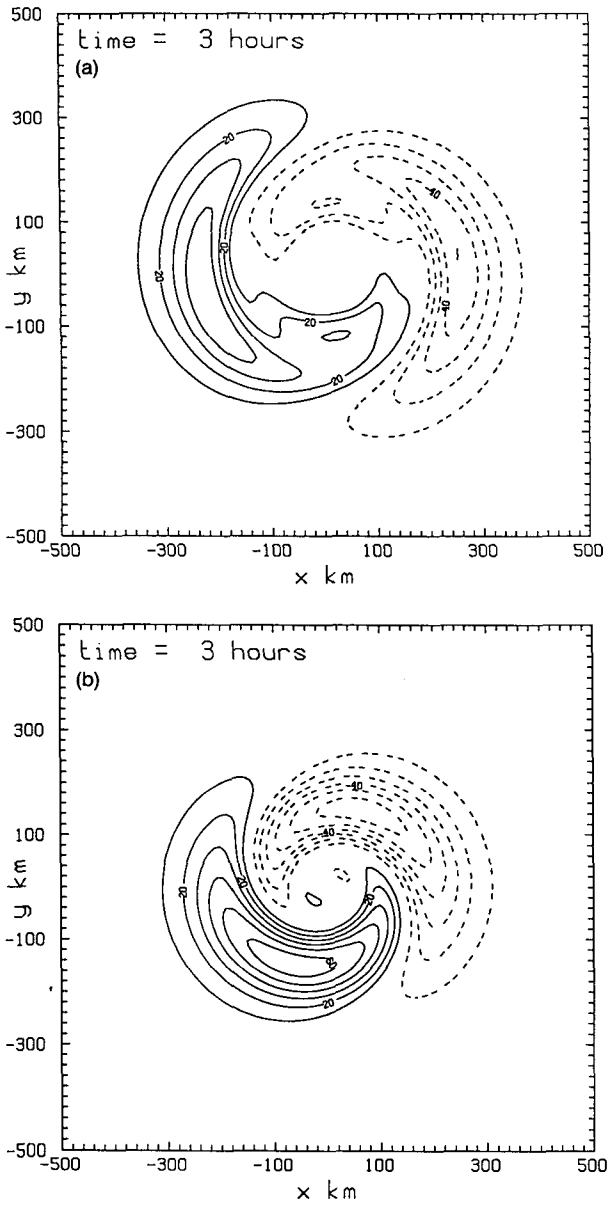

FIG. 6. Comparison of (a) the numerically and (b) analytically calculated vorticity asymmetries for the small vortex at 3 h.

(SUD, Fig. 8), but the radial gradient of symmetric vorticity is large in this region. Since the latter gradient changes sign at $r = 255$ km, the vorticity correction shows two outer gyres, a cyclonic one to the northwest and an anticyclonic one to the southeast. Each of these is symmetric about an axis in the direction of the relative streamflow at large distances. Furthermore, their sense of rotation implies a component of motion across vortex center towards the north-northeast.

At inner radii, the tendency to form an inner gyre with the opposite sense of rotation to the outer one is opposed by the strong shear of the tangential wind and,

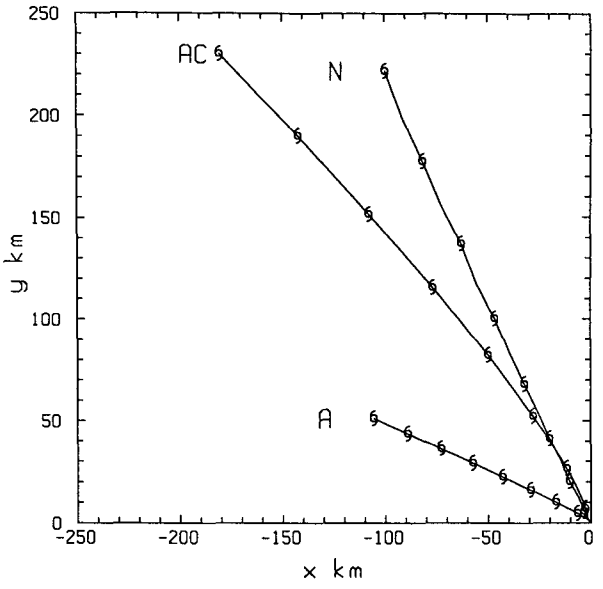

FIG. 7. Legend as for Fig. 5 except for small vortex in Fig. 1.

as in the case of the basic asymmetry discussed in section 2, the vorticity correction consists of alternate rings of positive and negative values. The radial scale of these rings decreases with time and their contribution to the streamfunction asymmetry rapidly becomes small in comparison to the outer gyres. The direction of the streamflow across the vortex center associated with the correction to the asymmetric vorticity field Γ_{ac} is evi-

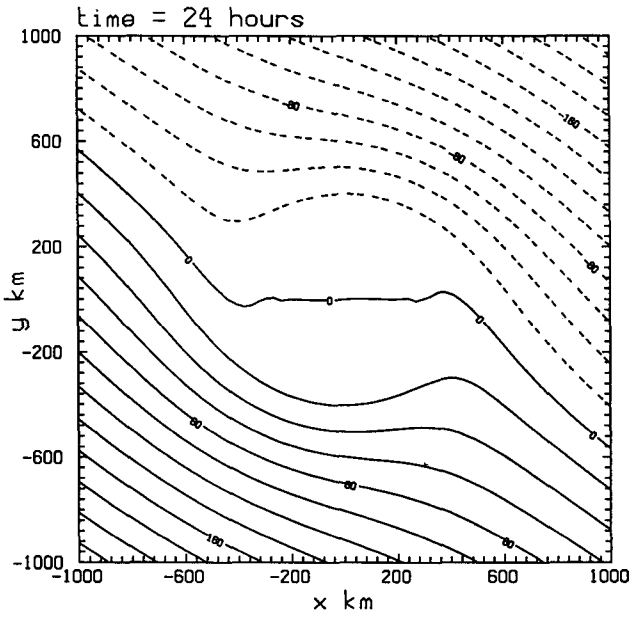

FIG. 8. Relative streamfunction Ψ'_a for the large vortex at 24 hours based on the zero order solution for Ψ_a and the vortex translation velocity at this order. Contour interval is 2×10^5 m^2 s^{-1}.

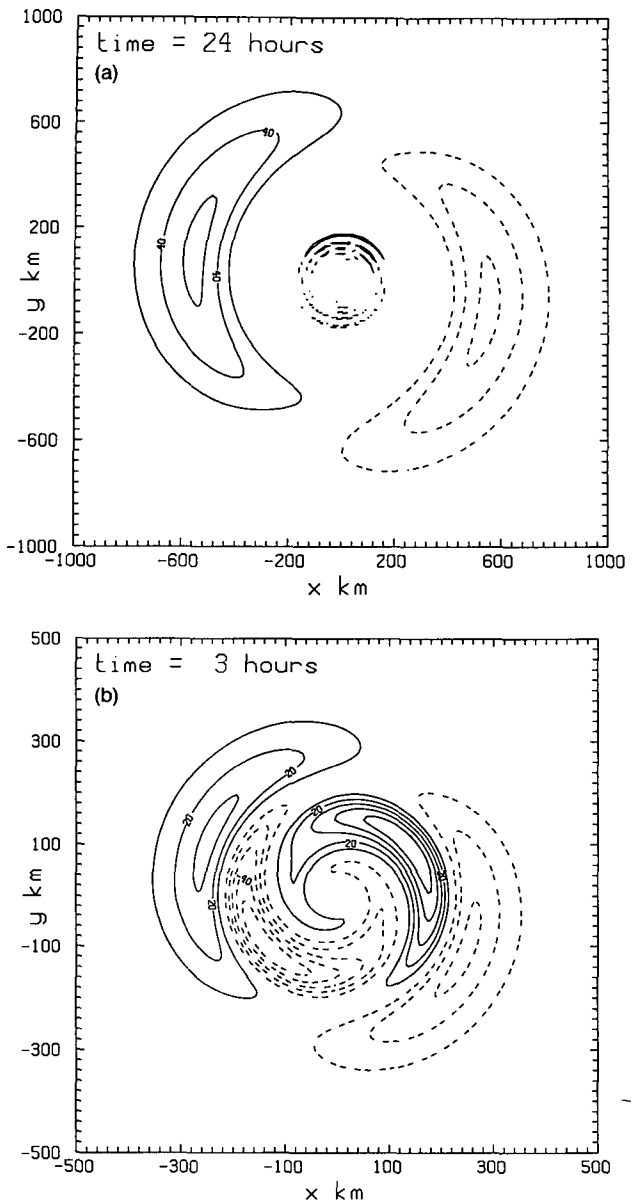

FIG. 9. Pattern of asymmetric vorticity correction Γ_{ac}: (a) for the standard vortex case at 24 hours; (b) for the small vortex at 3 h.

dently of the right sense to explain the discrepancy in the analytically computed vortex track. The vorticity correction for the small vortex at 3 hours is shown in Fig. 9b with the same contour interval as in Fig. 6. Note that the correction is even more significant in this case than in the standard vortex case at 24 hours.

The total vorticity asymmetries ($\Gamma_a + \Gamma_{ac}$) show excellent agreement with those obtained from the full numerical solution at least up to 24 hours (Fig. 10a,b). In particular, in the case of the small vortex, the corrected asymmetries show the subsequent retrograde rotation of the gyre asymmetry as discussed in section 2 (Fig. 10d). Note that the analytically calculated asymmetric gyres for the small vortex continue to show good agreement with the numerically computed ones at 12 h (Figs. 10e, f).

Consideration of the corrected vorticity patterns indicate why smaller vortices with the same radius of maximum tangential wind speed and same maximum tangential wind speed have a more northerly track than larger ones. It is because the term $-(\mathbf{U}-\mathbf{c})\cdot\nabla\zeta$ makes a proportionately larger contribution to the vortex asymmetry for smaller vortices, leading to a greater retrogression of the axis of the asymmetric gyres in these cases.

As in the zero order analysis, we can calculate the streamfunction correction corresponding with (3.10) and, in particular, the velocity correction $\Delta\mathbf{c}$ to the flow across the vortex center. In analogy with (2.12), it follows that

$$\Delta\mathbf{c} = \left[-\left.\frac{\partial\Psi_{2c}}{\partial r}\right|_{r=0}, \left.\frac{\partial\Psi_{1c}}{\partial r}\right|_{r=0} \right], \tag{3.13}$$

where

$$\left.\frac{\partial\Psi_{nc}}{\partial r}\right|_{r=1} = -\frac{1}{2}\int_0^\infty \zeta_{nc}(r,t)\,dr. \tag{3.14}$$

The corresponding track correction $\Delta x = (\Delta x, \Delta y)$ is then obtained by integrating (3.13) with respect to time in analogy with (2.11). The result is

$$\begin{bmatrix}\Delta x(t)\\ \Delta y(t)\end{bmatrix} = \frac{1}{4}\beta t^2 \int_0^\infty \frac{d\zeta}{dr}\,dr \int_0^r p\left(1-\frac{p^2}{r^2}\right)\begin{bmatrix}\gamma_1(r,p,t)\\ \gamma_2(r,p,t)\end{bmatrix}dp, \tag{3.15}$$

where

$$\gamma_1(r,p,t) = \frac{\sin\Omega_r - \Omega_r}{\Omega_r^2} - \frac{(\sin\Omega_r)/\Omega_r - (\sin\Omega_p)/\Omega_p}{\Omega_r - \Omega_p}, \tag{3.16a}$$

$$\gamma_2(r,p,t) = \frac{1-\cos\Omega_r}{\Omega_r^2} - \frac{(1-\cos\Omega_r)/\Omega_r - (1-\cos\Omega_p)/\Omega_p}{\Omega_r - \Omega_p}, \tag{3.16b}$$

with the notation that $\Omega_r = \Omega(r)t$ and $\Omega_p = \Omega(p)t$. The corrected tracks for the large and small vortices in Fig. 1 are shown in Figs. 5 and 7, respectively. The agreement is now excellent both in speed and direction at early times (at least 36 hours for the larger vortex and 12 hours for the smaller one) after which the analytically and numerically calculated tracks begin to diverge.

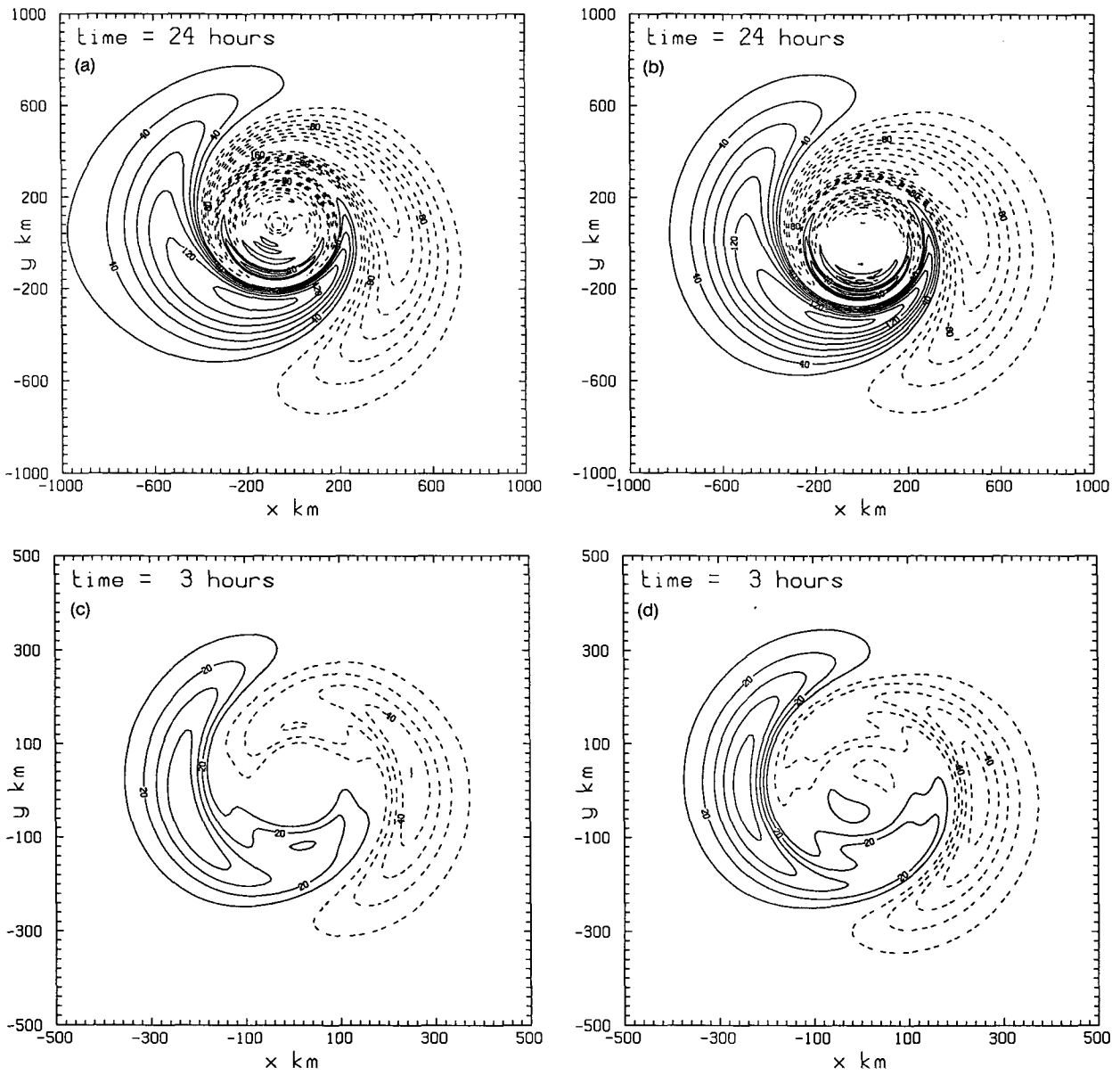

FIG. 10. Comparison of the analytically corrected vorticity asymmetry $\Gamma_a + \Gamma_{ac}$ (a), (b) for the standard vortex at 24 h; (c), (d) for the small vortex at 3 h; (e), (f) for the small vortex at 12 h. The left-hand panels are for the numerical calculation.

In the case of the larger vortex, the analytically computed track direction remains good, but the vortex speed is overestimated. In the smaller vortex case, the directions show a significant deviation also.

Figure 11 compares the streamfunction calculated from the analytical theory for the standard vortex at 24 hours with that for the numerical calculation. The former is obtained by adding the zero order streamfunction from (2.8) to the correction Ψ_{ac}, calculated by applying (2.8) and (2.9) to Eq. (3.10). The latter was calculated for a 4000 km $\times$ 4000 km domain and normalized to have zero value at the vortex center to enable a proper comparison to be made with the analytical solution. As for the vorticity field, the agreement is generally very good. In contrast to the analytical solution, the streamlines for numerical solution show a slight curvature on either side of the vortex center, presumably associated with the contribution of other wavenumbers to the vortex asymmetry (see below). However, the mean flow direction across the vortex center corresponds closely with that of the analytical solution, showing that the analytic theory captures the essentials of the vortex motion dynamics.

The ultimate breakdown of the analytical theory is

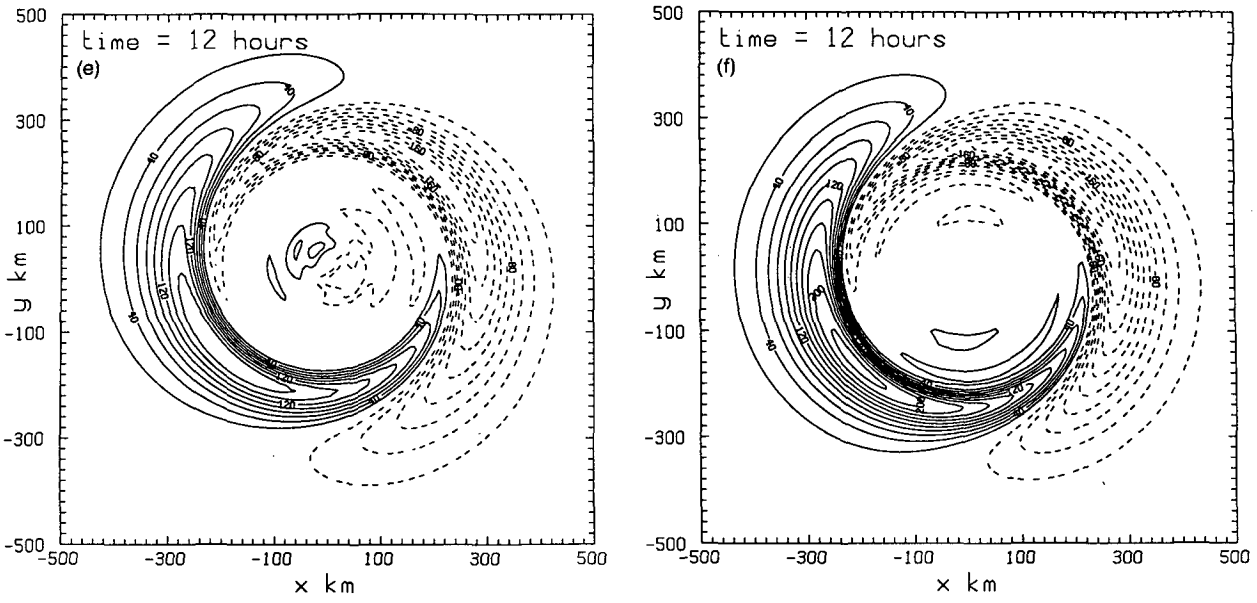

FIG. 10 (*Continued*)

presumably attributable to the linearization assumption implicit in the assumption that advective changes in vorticity occur following fluid parcels moving with the tangential velocity of the basic vortex about the local vortex center. As the vortex speed is at most a few meters per second, the latter is a good approximation within two or three hundred kilometers of the center for the vortices studied, but it is not valid at large radii where tangential speeds are comparable with, or even smaller than the vortex speed. This is illustrated in the case of the larger vortex in Fig. 12 which shows the trajectories of selected particles relative to the vortex center calculated from the full numerical solution. Ultimately, the vorticity changes experienced by particle motions at radii where $V(r)$ is not overwhelmingly larger than the vortex speed contribute significantly to the coherent part of the asymmetric vorticity field (see SUD, §4).

It is interesting to note that the breakdown of the theory cannot be delayed by including the second term, $-(\mathbf{U}-\mathbf{c})\cdot\nabla f$, on the right hand side of Eq. (3.3). It is straightforward to show that, when estimated using the zero-order solution, this term projects partly on to a symmetric component and partly on to a wavenumber-two asymmetry (see Appendix B). The symmetric component cannot induce a flow across the vortex center, of course, and it can be shown that this is true also of the wavenumber-two asymmetry. In a method of partitioning where "the vortex" is *defined* as the symmetric component of the flow at any instant, as used for example by Fiorino and Elsberry (1989), the symmetric part of the term, $-(\mathbf{U}-\mathbf{c})\cdot\nabla f$, would contribute to a change in the vortex profile with time. Indeed, in the present analysis, this is the only term that contributes to such a change, since the azimuthal averages of Ψ'_a and Ψ_{ac} ($=\Psi_{1c}\cos\theta+\Psi_{2c}\sin\theta$) are identically zero.

4. The "bogussing" problem

Tropical cyclones are generally in scale well below the resolution of the conventional data observing network and their presence may be missed entirely by a straight forward objective analysis of the data. Accordingly it may be necessary to insert a so-called "bogus vortex" in the analysis in preparation for the initialization of a forecast model. Ideally the bogus vortex should correspond with the estimated size and intensity of the cyclone. Moreover, one would wish that, when assimilated into the model, the bogus vortex would move initially at least with the observed speed and direction of the cyclone. It is clear from the results of the prototype problem that an initially symmetric bogus vortex will develop its own asymmetries and that these will influence its subsequent motion. The case of vortices initialized in spatially varying environmental flows is studied in Ulrich and Smith (1990). Therefore, it would seem desirable to initialize a model with an asymmetric vortex, chosen to ensure that the model cyclone has the initial speed and direction of that observed. In the absence of an environmental flow, one could use the present analytical solution to calculate an appropriate asymmetric vortex such that the vortex velocity equals the observed speed and direction of the cyclone. One would have to select (arbitrarily) a time at which to do this and the effectiveness of the initial-

ization would depend on the sensitivity of the forecast to the time chosen. The method might be expected to retain some skill if the environmental flow is weak. We are investigating these problems currently and the results will be reported in due course. The important question of correctly initializing vortices in environmental flows with significant horizontal shear and in baroclinic models with vertical shear remains also to be addressed.

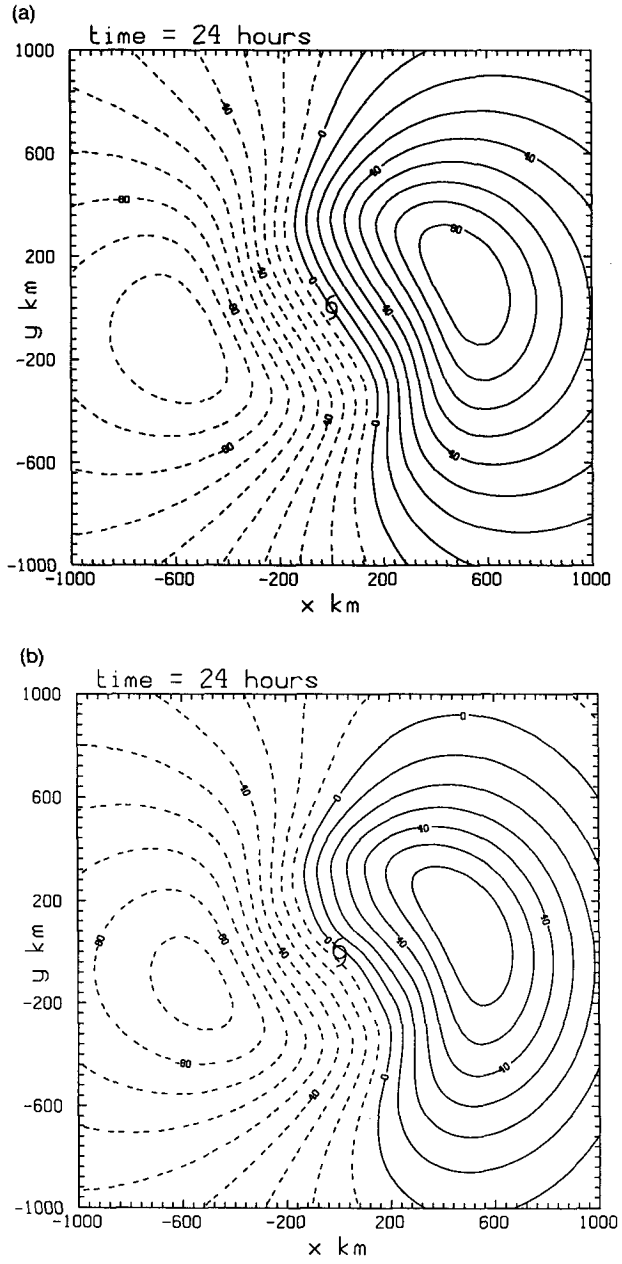

FIG. 11. (a) analytically corrected streamfunction asymmetry $\Psi_a + \Psi_{ac}$ for the standard vortex at 24 hours compared with (b) the corresponding field for the numerical solution. The numerical calculation was carried out on a 4000 × 4000 km domain. The part shown in (b) is centered on the vortex position at this time.

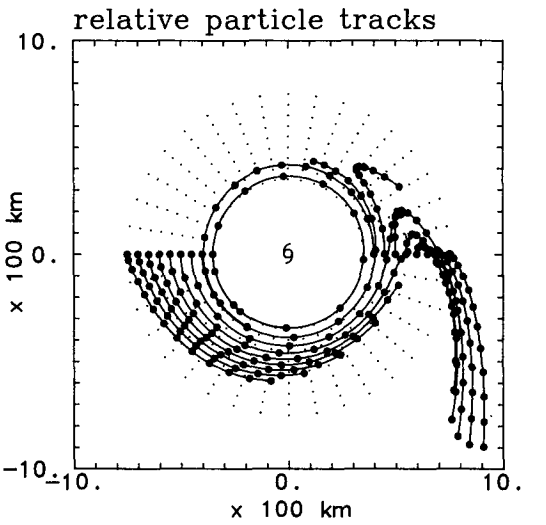

FIG. 12. Selected particle trajectories relative to the moving vortex in the numerical calculation for the standard vortex. The trajectories start along the x-axis. Thick dots indicate 6 hourly positions. Thin dots mark circular paths at the initial radii of particles.

5. Conclusion

The early motion of an initially symmetric barotropic vortex on a beta plane and the vortex asymmetries that accompany the motion can be accurately calculated using an essentially linear Lagrangian model in which relative vorticity changes are computed for particles moving in circular orbits relative to the moving vortex. The vortex motion is determined on the assumption that the vortex center, defined as the point of maximum relative vorticity, is advected by the asymmetric streamflow across it. For tropical cyclone scale vortices, the theory agrees closely with the results of analogous numerical calculations for a period between one and two days. Thereafter, the analytical and numerical model calculations steadily diverge, although for larger scale vortices the track directions continue to agree until at least 48 hours. The theory begins to break down as relative vorticity changes in particles at large distances from the vortex center begin to contribute significantly to the asymmetric vorticity distribution. Such particles have tangential velocities comparable with or less than the speed of vortex translation and accordingly their motion relative to the moving vortex deviates appreciably from a circular path as assumed by the theory.

Acknowledgments. We gratefully acknowledge partial support for this work from the U.S. Office of Naval Research through Grant N 00014-87-J-1250.

APPENDIX A

Derivation of Eq. (3.11)

Using (3.8) and (3.9), Eq. (3.4) can be written as

$$\frac{d\Gamma_{ac}}{dT} = \frac{1}{r}\frac{d\zeta}{dr}\left[\Psi'_2(r, t)\cos\theta - \Psi'_1(r, t)\sin\theta\right],$$

where d/dt denotes integration following a fluid parcel moving in a circular path of radius r about the vortex center with angular velocity $\Omega(r)$. It follows that

$$\Gamma_{ac} = \frac{1}{r}\frac{d\zeta}{dr}\int_0^t \left[\Psi'_2(r, t')\cos\theta(t') - \Psi'_1(r, t')\sin\theta(t')\right]dt',$$

where $\theta(t') = \theta - \Omega(r)(t - t')$. Using (3.7), this becomes

$$\Gamma_{ac} = \frac{1}{2}\frac{d\zeta}{dr}\int_0^t\int_0^r \left(1 - \frac{p^2}{r^2}\right) \times \left[\zeta_2(p, t')\cos\theta(t') - \zeta_1(p, t')\sin\theta(t')\right]dpdt',$$

and this reduces further on substitution for ζ_n from (2.7) and the above expression for $\theta(t')$ giving

$$\Gamma_{ac} = -\frac{1}{2}\beta\frac{d\zeta}{dr}\int_0^r p\left(1 - \frac{p^2}{r^2}\right) \times \int_0^t \left[\cos\{\theta - \Omega(r)(t - t')\} - \cos\{\theta - \Omega(r)(t - t') - \Omega(p)t'\}\right]dt'dp.$$

Equation (3.11) follows on integration with respect to t'.

APPENDIX B

Estimation of the Term $-(\mathbf{U} - \mathbf{c})\cdot\nabla f$ in Eq. (3.3)

Using (3.6) and noting that $(\partial/\partial x) = \cos\theta(\partial/\partial r) - \sin\theta(1/r)(\partial/\partial\theta)$,

$$-(\mathbf{U}_a - \mathbf{c})\cdot\nabla f = -\beta\left(\frac{\partial\Psi'_a}{\partial x}\right) = -\beta\left[\cos^2\theta\frac{\partial\Psi'_1}{\partial r} - \sin^2\theta\frac{\Psi'_1}{r} + \cos\theta\sin\theta\left(\frac{\partial\Psi'_2}{\partial r} - \frac{\Psi'_2}{r}\right)\right].$$

Substituting expressions for Ψ'_n and their derivatives from (3.7) gives after a little algebra:

$$-(\mathbf{U}_a - \mathbf{c})\cdot\nabla f = -\frac{1}{2}\beta\left[\int_0^r \zeta_1(p, t)dp + \frac{\cos2\theta}{r^2}\int_0^r p^2\zeta_1(p, t)dp + \frac{\sin2\theta}{r^2}\int_0^r p^2\zeta_2(p, t)dp\right].$$

The contribution to this term to the vorticity asymmetry correction through (3.3) may be readily calculated by the procedure outlined in Appendix A.

REFERENCES

Adem, J., 1956: A series solution for the barotropic vorticity equation and its application in the study of atmospheric vortices. *Tellus*, **8**, 364–372.

Carr, L. E., and R. T. Williams, 1989: Barotropic vortex stability to perturbations from axisymmetry. *J. Atmos. Sci.*, **46**, 3177–3191.

Chan, J. C., and R. T. Williams, 1987: Analytical and numerical studies of the beta-effect in tropical cyclone motion. Part I: Zero mean flow. *J. Atmos. Sci.*, **44**, 1257–1265.

Fiorino, M., and R. L. Elsberry, 1989: Some aspects of vortex structure related to tropical cyclone motion. *J. Atmos. Sci.*, **46**, 975–990.

Kasahara, A., 1957: The numerical prediction of hurricane movement with the barotropic model. *J. Meteor.*, **14**, 386–402.

——, and G. W. Platzmann, 1963: Interaction of a hurricane with a steering field and its effect upon the hurricane trajectory. *Tellus*, **15**, 321–335.

Gent, P. R., and J. C. McWilliams, 1986. The instability of barotropic circular vortices. *Geophys. Astrophys. Fluid Dyn.*, **35**, 209–233.

Sasaki, Y., 1955: Barotropic forecasting for displacement of a typhoon. *J. Meteor. Soc. Japan*, **32**, 1–8.

——, and K. Miyakoda, 1954: Numerical forecasting of the movement of cyclone. *J. Met. Soc. Japan*, **32**, 9–19.

Shapiro, L. J., and K. V. Ooyama, 1990: Barotropic vortex evolution on a beta plane. *J. Atmos. Sci.*, **47**, 170–187.

Smith, R. K., W. Ulrich and G. Dietachmayer, 1990: A numerical study of tropical cyclone motion using a barotropic model. Part I: The role of vortex asymmetries. *Quart. J. Roy. Meteor. Soc.*, **116**, 337–362.

Ulrich, W., and R. K. Smith, 1989: A numerical study of tropical cyclone motion using a barotropic model. Part II: Spatially-varying large-scale flows. Submitted to *Quart. J. Roy. Meteor. Soc.*, **117**, in press.

Willoughby, H. E., 1989: Linear motion of a shallow-water, barotropic vortex. *J. Atmos. Sci.*, **45**, 1906–1928.